



AMS
American Meteorological Society

Supplemental Material

[© Copyright 2018 American Meteorological Society](#)

Permission to use figures, tables, and brief excerpts from this work in scientific and educational works is hereby granted provided that the source is acknowledged. Any use of material in this work that is determined to be “fair use” under Section 107 of the U.S. Copyright Act or that satisfies the conditions specified in Section 108 of the U.S. Copyright Act (17 USC §108) does not require the AMS’s permission. Republication, systematic reproduction, posting in electronic form, such as on a website or in a searchable database, or other uses of this material, except as exempted by the above statement, requires written permission or a license from the AMS. All AMS journals and monograph publications are registered with the Copyright Clearance Center (<http://www.copyright.com>). Questions about permission to use materials for which AMS holds the copyright can also be directed to permissions@ametsoc.org. Additional details are provided in the AMS Copyright Policy statement, available on the AMS website (<http://www.ametsoc.org/CopyrightInformation>).

1 **Supplementary Online Material to**
2 **Climate responses to aerosol geoengineering: a multi-method comparison**

3 Authors: Helene Muri^{1,2}, Jerry Tjiputra³, Odd Helge Otterå³, Muralidhar Adakudlu³, Siv K.
4 Lauvset³, Alf Grini⁴, Michael Schulz⁴, Ulrike Niemeier⁵, Jón Egill Kristjánsson^{1,†}

5 Affiliations:

6 ¹University of Oslo, Department of Geosciences, Section for Meteorology and Oceanography,
7 Oslo, Norway

8 ²Norwegian University of Science and Technology, Department of Energy and Process
9 Engineering, Industrial Ecology Program, Trondheim, Norway

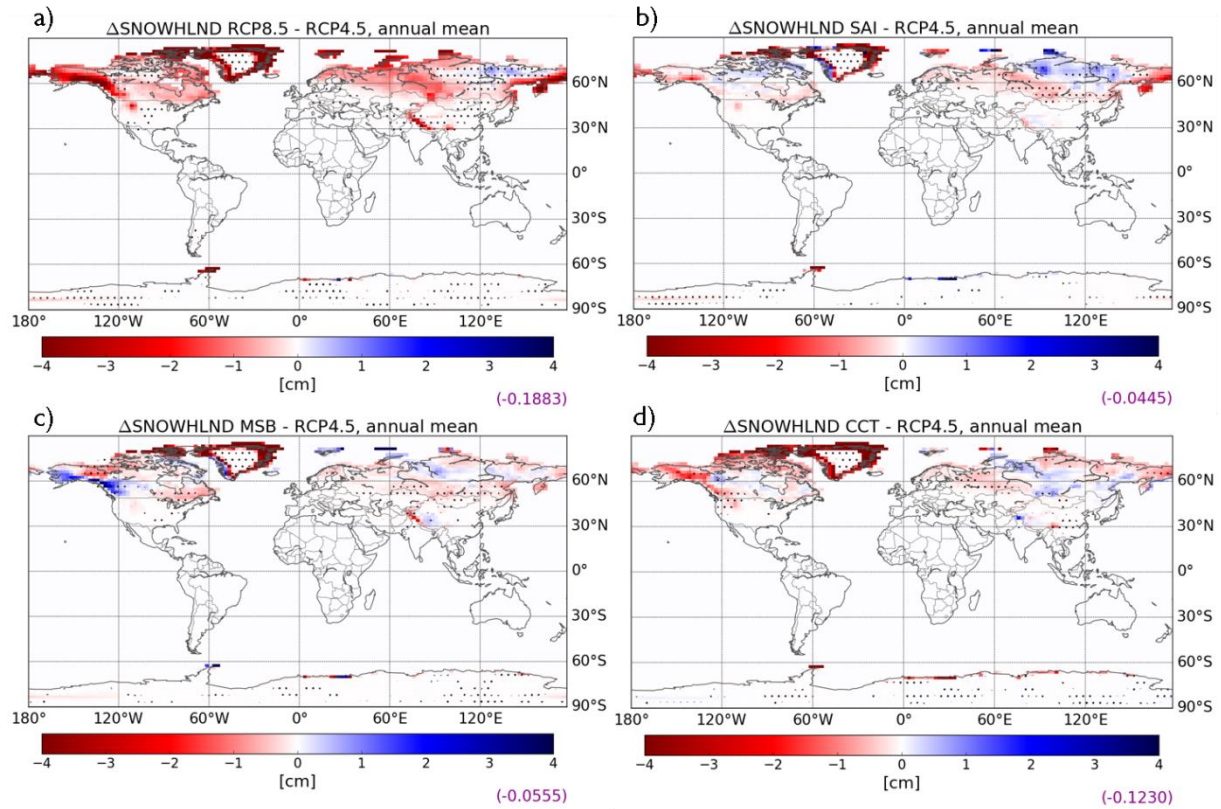
10 ³Uni Research Climate, Bjerknes Centre for Climate Research, Bergen, Norway

11 ⁴Meteorological Institute, Oslo, Norway

12 ⁵Max Planck Institute for Meteorology, Hamburg, Germany

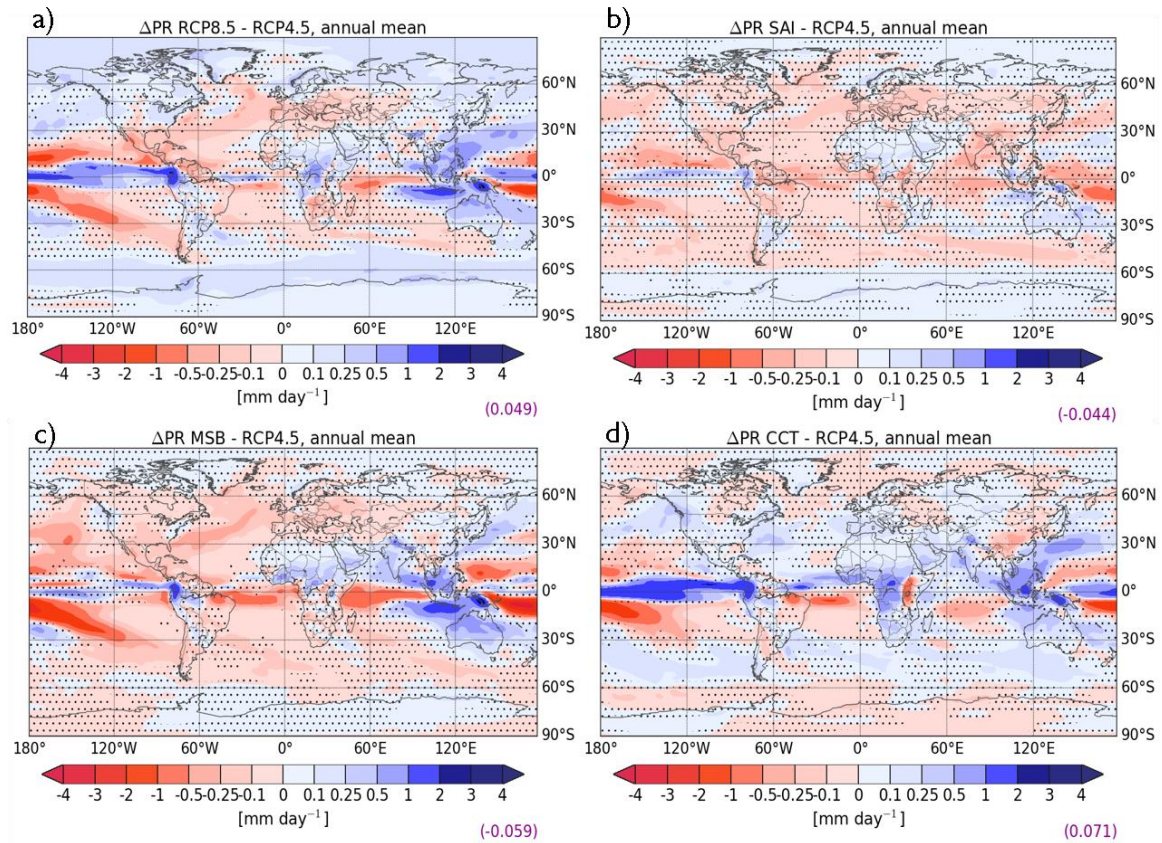
13 Corresponding author: helene.muri@ntnu.no

14



15

16 Figure S1: Annual mean land snow depth difference from RCP4.5 [cm]; a) RCP8.5, b)
 17 *RCP8.5+SAI*, c) *RCP8.5+MSB*, and d) *RCP8.5+CCT*. Means over all three ensemble member
 18 for each experiment over years 2060-2089. Non-stippling indicates a confidence level higher
 19 than 95% following Student's t-test. Global mean values in purple.



20

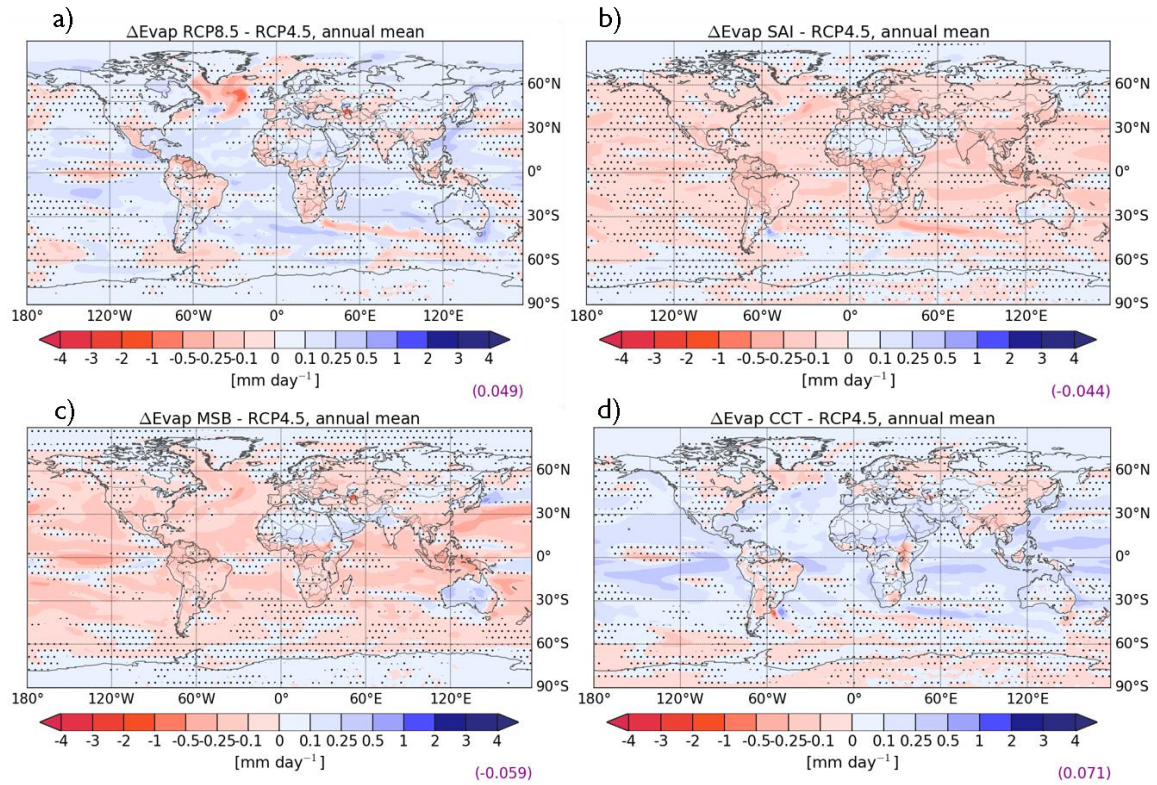
21 Figure S2: Annual mean precipitation rate difference [mm day⁻¹] from RCP4.5; a) RCP8.5, b)

22 RCP8.5+SAI, c) RCP8.5+MSB, and d) RCP8.5+CCT. Means over all three ensemble member

23 for each experiment over years 2060-2089. Non-stippling indicates a confidence level higher

24 than 95% following Student's t-test. Global mean values in purple.

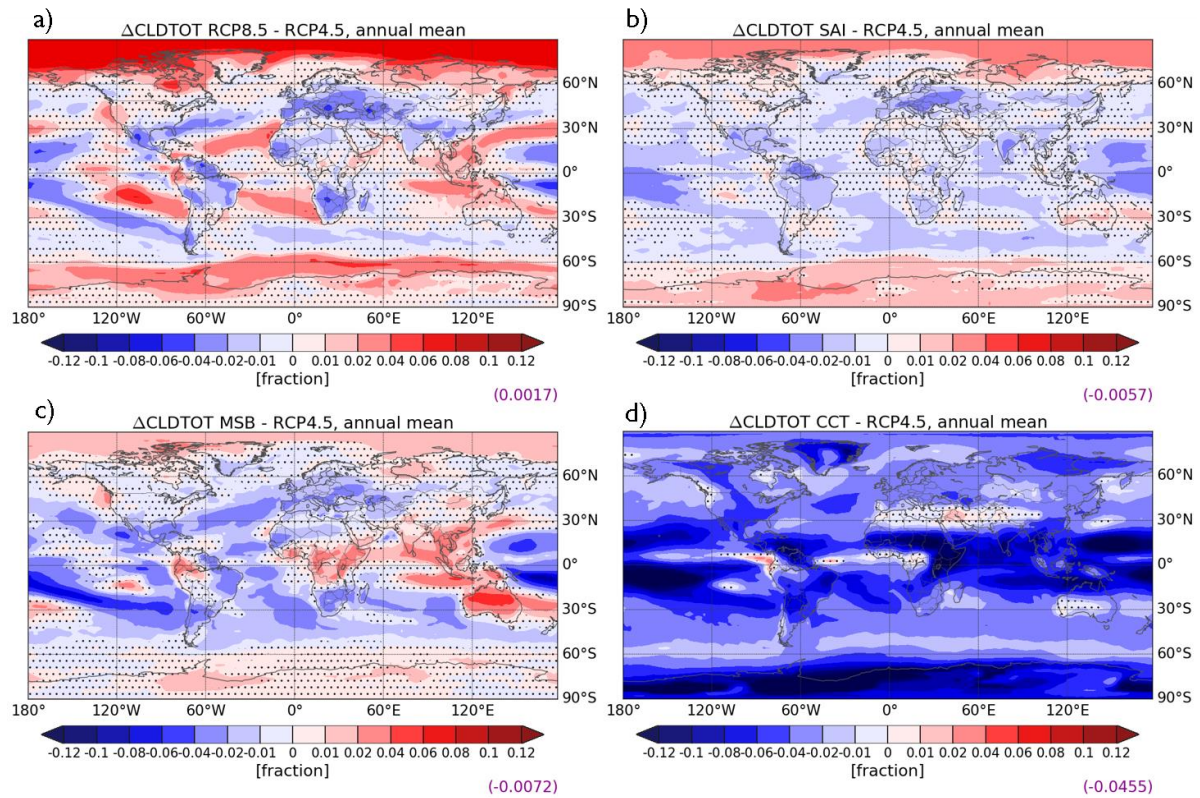
25



26

27 Figure S3: Annual mean evaporation rate difference [mm day^{-1}] from RCP4.5; a) RCP8.5, b)
 28 *RCP8.5+SAI*, c) *RCP8.5+MSB*, and d) *RCP8.5+CCT*. Means over all three ensemble member
 29 for each experiment over years 2060-2089. Non-stippling indicates a confidence level higher
 30 than 95% following Student's t-test. Global mean values in purple.

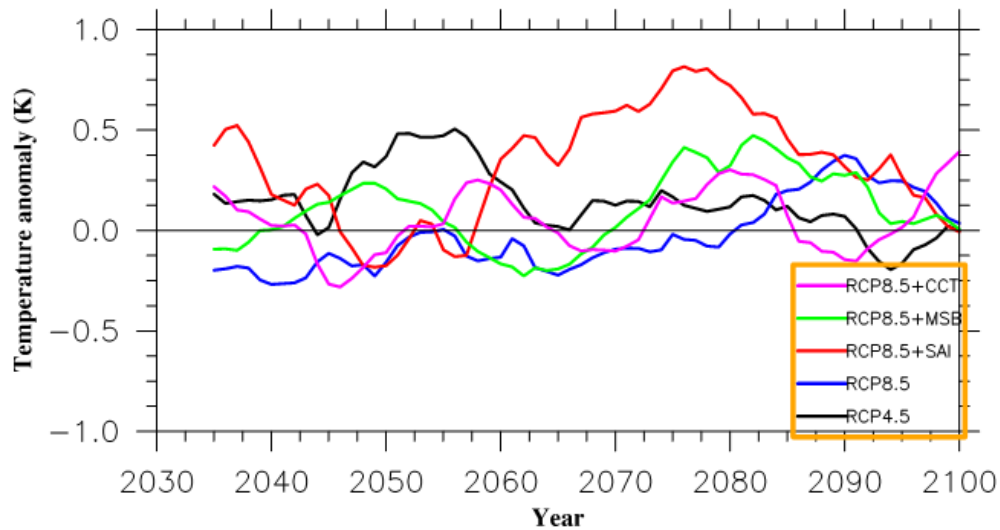
31



32

33 Figure S4: Annual mean total cloud fraction difference from RCP4.5 [fraction]; a) RCP8.5, b)
 34 *RCP8.5+SAI*, c) *RCP8.5+MSB*, and d) *RCP8.5+CCT*. Means over all three ensemble member
 35 for each experiment over years 2060-2089. Non-stippling indicates a confidence level higher
 36 than 95% following Student's t-test. Global mean values in purple.

37

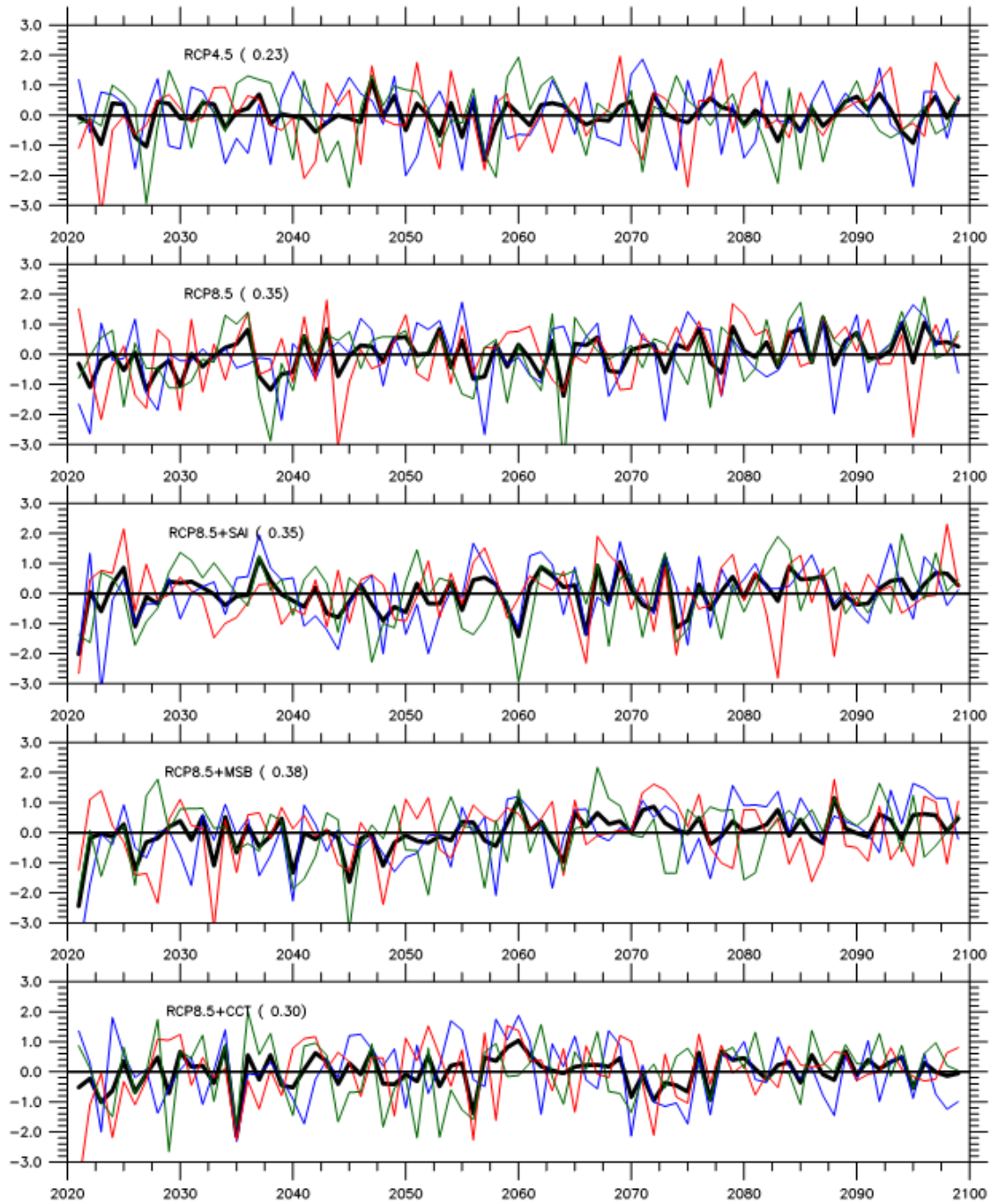


38

39 Figure S5: The ensemble mean 12-month running average of de-trended monthly temperature
40 anomalies [K] at 50 hPa averaged between 30°S – 30°N for different experiments. Black
41 curve: RCP4.5, blue: RCP8.5, red: *RCP8.5+SAI*, green: *RCP8.5+MSB* and pink:
42 *RCP8.5+CCT* (note: different colour from previous plots).

43

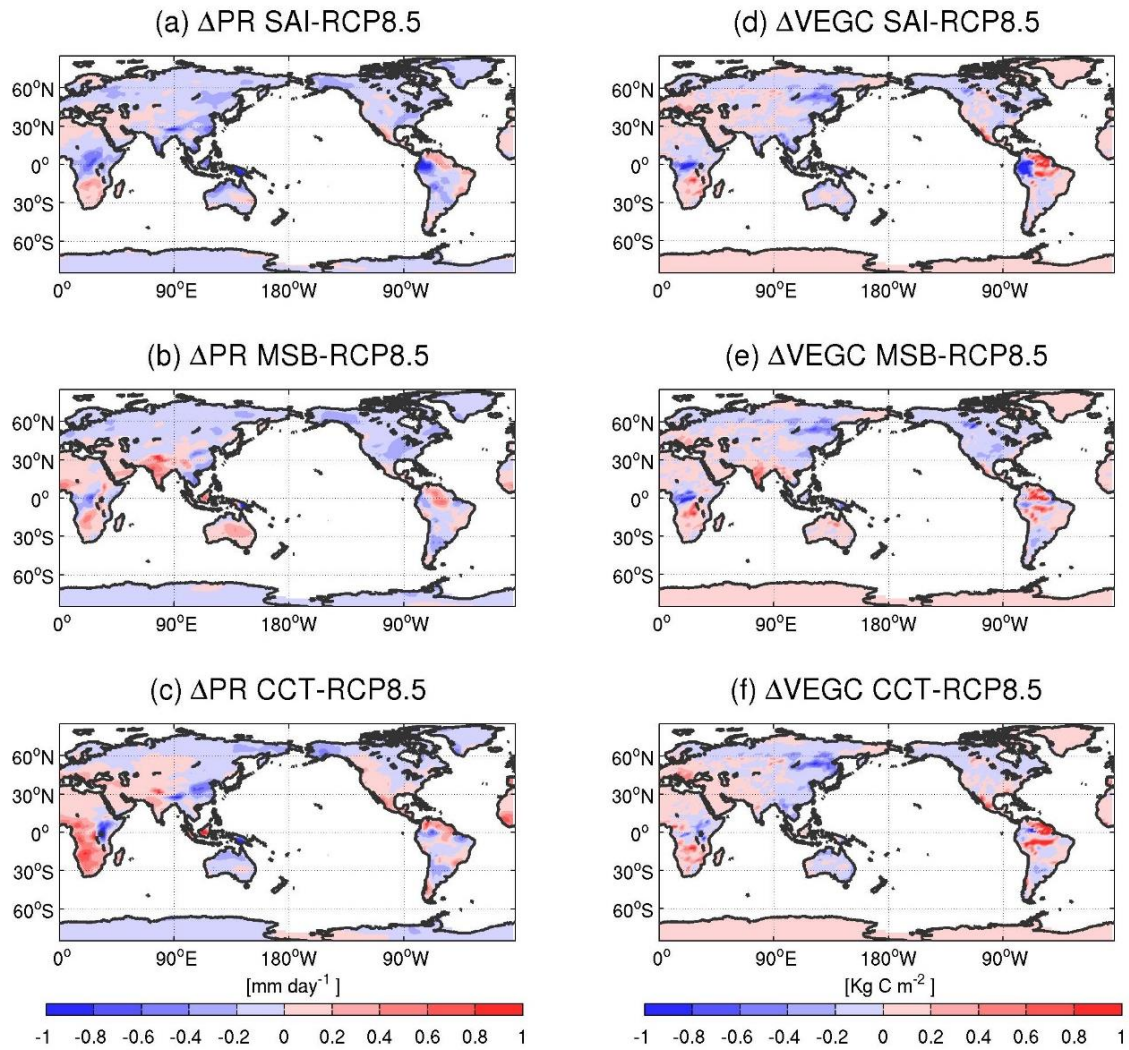
44 The NAO index, obtained by projecting the monthly winter MSLP anomalies onto the first
45 corresponding EOF mode, has an inter-annual variance of 0.23 in the RCP4.5 case (Figure S6).
46 The variance increases roughly by 50% in the RCP8.5 case following the global warming. The
47 aerosol injection geoengineering scenarios do not appear to have a strong influence on the
48 variance of the NAO index.



49

50 Figure S6: Standardized principal component time series indicating the inter-annual
51 variability of the NAO index. Thin coloured lines correspond to individual ensemble
52 members and the thick black line indicates the ensemble mean. The numbers inside the
53 parenthesis represent the inter-annual variance.

54



55 Figure S7: Annual mean difference of precipitation on land from RCP8.5 [mm day^{-1}]; a)
 56 *RCP8.5+SAI*, b) *RCP8.5+MSB*, and c) *RCP8.5+CCT*. Panels d-f vegetation carbon contents
 57 [kg C m^{-2}] from the respective experiments.
 58